# Synergistic Combinations of Multiple Chemotherapeutic Agents in High Capacity Poly(2-oxazoline) Micelles

Yingchao Han,[†,‡,§] Zhijian He,[†,§] Anita Schulz,[‖] Tatiana K. Bronich,[†] Rainer Jordan,[‖] Robert Luxenhofer,*[‖] and Alexander V. Kabanov*[†,⊥]

[†]Center for Drug Delivery and Nanomedicine and Department of Pharmaceutical Sciences, College of Pharmacy, University of Nebraska Medical Center, Omaha, Nebraska 68198-5830, United States

[‡]Biomedical Materials and Engineering Center, Wuhan University of Technology, Wuhan 430070, P. R. China

[‖]Professur für Makromolekulare Chemie, Department Chemie, Technische Universität Dresden, Zellescher Weg 19, 01069 Dresden, Germany

[⊥]Laboratory of Chemical Design of Bionanomaterials, Faculty of Chemistry, M. V. Lomonosov Moscow State University, Moscow 119992, Russia

Ⓢ Supporting Information

**ABSTRACT:** Many effective drugs for cancer treatment are poorly water-soluble. In combination chemotherapy, needed excipients in additive formulations are often toxic and restrict their applications in clinical intervention. Here, we report on amphiphilic poly(2-oxazoline)s (POx) micelles as a promising high capacity delivery platform for multidrug cancer chemotherapy. A variety of binary and ternary drugs combinations of paclitaxel (PTX), docetaxel (DTX), 17-allylamino-17-demethoxygeldanamy-cin (17-AAG), etoposide (ETO) and bortezomib (BTZ) were solubilized in defined polymeric micelles achieving unprecedented high total loading capacities of up to 50 wt % drug per final formulation. Multidrug loaded POx micelles showed enhanced stability in comparison to single-drug loaded micelles. Drug ratio dependent synergistic cytotoxicity of micellar ETO/17-AAG was observed in MCF-7 cancer cells and of micellar BTZ/17-AAG in MCF-7, PC3, MDA-MB-231 and HepG2 cells.



**KEYWORDS:** *block copolymer, combination therapy, drug delivery, drug formulation, nanomedicine, polymeric micelles, synergistic cytotoxicity*
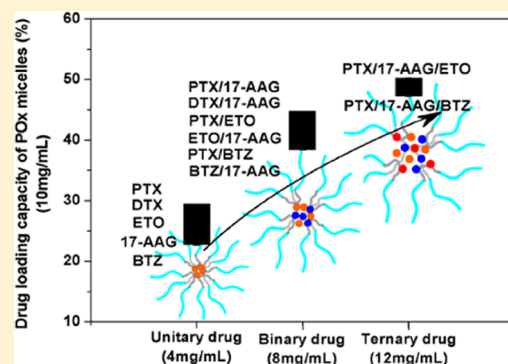
## 1. INTRODUCTION

Single drug therapy of cancer is rarely successful due to inherent and developing drug resistance of tumors. Even those tumors that initially respond to such therapy subsequently nearly inevitably adopt resistance by generating inhibitors against apoptotic stimuli or activating multidrug resistant genes (e.g., MDR1).[1] Furthermore, most tumors comprise heterogeneous cell populations and are sustained in growth by small populations of "tumor initiating cells" (TICs), which have high proliferation potential and are inherently resistant.[2−5] Survival of TICs during chemotherapy can result in tumor progression and recurrence. Thus clinical use of combination chemotherapies became a standard of treatment for most types of cancers.[6−9] Such therapy regimens commonly involve sequential administration of multiple drugs that can act along different and synergistic pathways and kill cancer cells better. Combining such drugs in one vehicle could simplify treatments and make it less hazardous to patients. Yet, many drugs are incorporated in different vehicles that are often incompatible with each other. Therefore, common vehicles that include multiple drugs are needed for next generation therapies.

Some researchers have sought such multidrug delivery systems. For instance, micelles of stearate-grafted chitosan oligosaccharide (CSO-SA) were used for codelivery of paclitaxel (PTX) and doxorubicin.[10] Another study employed nanoparticles of poly(D,L-lactide-co-glycolide acid) (PLGA) for simultaneous delivery of vincristine (VCR) and verapamil (VRP).[11] A liposomal delivery formulation for quercetin and VCR was also developed.[12] Additionally, Kwon et al. reported that poly(ethylene glycol)-*block*-poly(D,L-lactic acid) (PEG-*b*-PLA) micelles can deliver multiple drugs including combinations of PTX/17-allylamino-17-demethoxygeldanamycin (17-AAG), etoposide (ETO)/17-AAG, docetaxel (DTX)/17-AAG and PTX/ETO/17-AAG.[13]

To make this approach practical and translate it to clinic the multidrug vehicles must be safe to patients and have high loading capacity with respect to multiple drugs. The latter
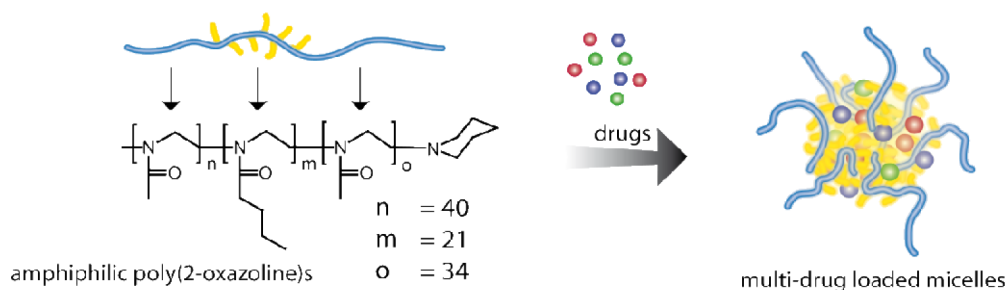
**Figure 1.** Chemical structure of amphiphilic POx copolymer, P(MeOx$_{40}$-*b*-BuOx$_{21}$-*b*-MeOx$_{34}$), and schematic representation of multiple drug loaded micelles.

remains a principal limitation for most drug delivery systems carrying water-insoluble drugs. For example, loading capacities of most polymeric micelle systems for water-insoluble drugs do not exceed 10 to 15% by weight of the dispersed phase.[14] Such mediocre loading can be an impediment for even a single drug formulation, while for a multidrug vehicle it becomes a principal roadblock to pharmaceutical development. Since treatment doses in chemotherapeutic regimens cannot be significantly altered, the low loading of multiple drugs would require using prohibitively high doses of the vehicle proper, which could result in the vehicle-derived toxicity. A well-known example of dose limiting vehicle toxicity is Taxol, a clinical formulation of PTX, which contains as excipient Cremophor EL (PEGylated castor oil) that can induce hypersentitive reactions as well as neuro- and nephrotoxicities during iv infusions.[15−17]

Therefore, in an attempt to develop a multidrug vehicle this work focused on polymeric micelles of amphiphilic poly(2-oxazoline) (POx) block copolymers that were recently shown to have an unprecedented high loading capacity for PTX of up to 45 wt %.[14] POx has attracted increasing interest for biomedical applications due to their tunable properties and structure, which compare favorably to polyethers, such as PEG.[18,19] The POx backbone with pending amide moieties is highly hydrated while the alkyl side chains of varying length can provide for amphiphilic character of the monomer units (nonionic polysoap) and determine the water solubility of the polymer.[20] Variation of the length of the alkyl side chain in POx allows fine-tuning the hydrophilic−lipophilic balance of each monomer unit, as well as of the entire polymer chain. For example, a short side chain POx, poly(2-methyl-2-oxazoline) (PMeOx), is highly hydrophilic while poly(2-ethyl-2-oxazoline) (PEtOx) shows some amphiphilicity, comparable to PEG,[21,22] and displays a temperature-dependent water solubility (lower critical solution temperature).[23,24] Both PMeOx and PEtOx exhibit stealth properties and biodistribution similar to PEG when administered alone or grafted onto liposomes.[21,25−27] Poly(2-propyl-2-oxazoline) displays lower critical solution temperature around 25 °C (*n*-propyl) and 47 °C (*i*-propyl).[28,29] Poly(2-butyl-2-oxazoline) (PBuOx) is water-insoluble at room temperature and suitable to build a hydrophobic block in POx block copolymers, in which PMeOx or PEtOx are used as hydrophilic blocks. Such block copolymers form stable polymeric micelles, and their interaction with biological entities (e.g., rate of endocytosis) can be fine-tuned through the polymer structure.[30] We have recently shown that the PBuOx core of such micelles can efficiently incorporate PTX. As a result, drug-containing aggregates of defined size are produced, in which the drug can comprise nearly half of the aggregate mass.[14] These PTX-

loaded POx micelles remained stable throughout lyophilization/redispersion cycles and exhibited low toxicity and complement activation.

This paper addresses two principal new questions (Figure 1): first, whether different multiple water-insoluble drugs can be simultaneously incorporated into such POx micelles with high loading capacity preserved, and second, whether these drugs can be combined in one POx micelle formulation to form pharmacologically synergistic chemotherapeutic combinations of high potency to kill cancer cells. The results suggest that POx micelles are a promising high-capacity multidrug delivery platform for combination cancer chemotherapy.

## 2. MATERIALS AND METHODS

**2.1. Materials.** The amphiphilic triblock copolymers [batch 1, P(MeOx$_{40}$-*b*-BuOx$_{21}$-*b*-MeOx$_{34}$), $M_n$ = 9.1 kg/mol, $Đ_M$ ($M_w$/$M_n$) = 1.14; batch 2, P(MeOx$_{33}$-*b*-BuOx$_{26}$-*b*-MeOx$_{45}$), $M_n$ = 10.0 kg/mol, $Đ_M$ = 1.14] were synthesized as described in the previous study.[14] PTX, DTX, 17-AAG and bortezomib (BTZ) were purchased from LC Laboratories (Woburn, MA). ETO was obtained from Sigma-Aldrich Inc. (St. Louis, MO). Alexa Fluor 647 (AF 647)-*N*-hydroxysuccinimide (NHS) ester labeling kits (A20173) and BODIPY FL PTX (P7500) were purchased from Invitrogen. All other materials were from Fisher Scientific Inc. (Fairlawn, NJ), and all reagents were HPLC grade (see all drug structures in Figure S1 in the Supporting Information). The MCF-7 (HTB-22), PC3 (CRL-1435), HepG2 cells (HB-8065) and MDA-MB-231 (HTB-26) were originally obtained from ATCC. Cells were cultured in DMEM medium (Gibco 11965-092) supplemented with 10% FBS and 1% penicillin−streptomycin.

**2.2. Methods.** *2.2.1. Preparation of Drug Loaded POx Micelles.* Drug loaded POx micelles were prepared using the film hydration method.[14] Predetermined amounts of POx and drugs (stock solution 10−20 g/L in ethanol) were combined with small amount of ethanol and mixed well. Following removal of ethanol (40 °C, air flow), the formed thin film was further dried *in vacuo* to remove residual solvent. The dried film was subsequently redispersed with appropriate amounts of deionized (DI) water and heated at 50−60 °C for 5−20 min (heating time dependent on the drug concentration; for example, 5 min for low concentration and up to 20 min for high concentration) to procure drug loaded polymeric micelles. POx micelles coloaded with multiple drugs were prepared accordingly with final polymer concentration of 10 g/L and each drug concentration of 4 g/L. Samples were allowed to cool to room temperature and centrifuged at 10,000 rpm (9630*g*) for 3 min (Sorvall Legend Micro 21R Centrifuge, Thermo

Scientific) to remove residual solid. Only the transparent supernatant was used for the following experiments.

### 2.2.2. High Performance Liquid Chromatography (HPLC) Analysis of Drugs in POx Micelles.

The amounts of drugs solubilized in POx micelles were quantified via reverse-phase HPLC using an Agilent Technologies 1200 series HPLC system using a Nucleosil C18 5 $\mu$m column (250 mm × 4.6 mm). The sample was diluted 20 times using mobile phase (specified below) and injected (20 $\mu$L) into the HPLC system. For PTX, 17-AAG and the combination of PTX/17-AAG, a mixture of acetonitrile (ACN)/methanol (MeOH)/water (39/38/23, v/v/v) was used as mobile phase. The retention times of PTX and 17-AAG were 5.0 and 7.1 min respectively. Similarly, ACN/water (55/45, v/v) was applied for DTX, 17-AAG and DTX/17-AAG. The flow rate was 1.0 mL/min, and column temperature was 30 °C. Detection wavelength was 227 nm for PTX and DTX, and 333 nm for 17-AAG. The retention times of DTX and 17-AAG were 8.1 and 13.3 min respectively. For all ETO-containing samples, a stepwise gradient was used. First, the analyte was eluted for 10 min with ACN/MeOH/water (0.1% phosphoric acid, 1% MeOH) (5/5/90, v/v/v) followed by a second 10 min elution of ACN/water (0.1% phosphoric acid, 1% MeOH) at a ratio of 60/40 (1 min transition). Column temperature was 40 °C, and detection wavelength for ETO was 227 nm. Under these conditions, the retention times of ETO, PTX and 17-AAG were 9.1, 16.9 and 18.7 min, respectively. Accordingly, for samples containing BTZ, another two-step gradient was applied: ACN/water (0.1% phosphoric acid) 90/10 (v/v) for the first minute; and ACN/MeOH/water (0.1% phosphoric acid) 35/35/30 (v/v/v) for the following 10 min. The flow rate was 2.0 mL/min, and column temperature was 55 °C. Detection was performed at 270 nm for BTZ. The retention times of PTX, 17-AAG and BTZ were 1.5, 1.7 and 3.6 min respectively.

### 2.2.3. Drug loading calculations.

The following equations were used to determine drug loading capacity (LC), loading efficiency (LE) and drug loading (DL):

$$LC = \frac{m_{drug}}{m_{drug} + m_{excipient}} \times 100\% \tag{1}$$

$$LE = \frac{m_{drug}}{m_{drug\ added}} \times 100\% \tag{2}$$

$$DL = \frac{m_{drug}}{m_{excipient}} \times 100\% \tag{3}$$

where $m_{drug}$ and $m_{excipient}$ are the weight amounts of the solubilized drug and polymer excipient in the dispersion, while $m_{drug\ added}$ is the weight amount of the drug added to the dispersion.

### 2.2.4. Dynamic Light Scattering (DLS).

The size distribution of micelles was investigated with DLS using a Nano-ZS (Malvern Instruments Inc., U.K.). The sample was diluted 10 times with DI $H_2O$ to yield 1 g/L final polymer concentration prior to the measurement. The intensity-mean $z$-averaged particle size (effective diameter) and the polydispersity index (PDI) obtained from cumulant analysis were given to reflect hydrodynamic diameters of drug loaded POx micelles. Measurements were repeated over prolonged time periods in order to evaluate stability of drug loaded micelles.

### 2.2.5. Atomic Force Microscopy (AFM).

One drop of the polymeric micelle solution (diluted 100-fold with DI $H_2O$) was deposited on negatively charged surface of freshly cleaved mica. After approximately two minutes, the sample was washed with a few drops of DI water and dried under argon atmosphere. AFM scans were acquired at ambient conditions with a MultiMode NanoScope IV system [Veeco (DI), Santa Barbara, CA, USA] using tapping mode. The obtained scans were analyzed using Femtoscan software.

### 2.2.6. Drug Release Studies.

The drug release from POx micelles was studied using membrane dialysis method against phosphate buffered saline (PBS, pH 7.4) at 37 °C. Briefly, the drug loaded POx micelle formulations were diluted with PBS to yield solutions of approximately 0.1 mg/mL of each drug. Then the resulting solutions (100 $\mu$L) were placed in 100 $\mu$L floatable Slide-A-Lyzer MINI dialysis devices with a MWCO of 3.5 kDa (Thermo Scientific) and suspended in 20 mL of PBS. One device was used for every time point. At each time point the sample was withdrawn from the dialysis device and the remaining drug amount of sample was quantified by HPLC. The experiments were carried out in triplicate. The experiment setup ensured that the sink conditions were realized. The solubility of the least soluble drug (PTX) in PBS is ca. 1 $\mu$g/mL. Thus at 100% release the maximal concentration of PTX (0.5 $\mu$g/mL) would still be below the solubility limit.

### 2.2.7. Confocal Laser Scanning Microscopy (CLSM).

POx was labeled with AF647 according to the manufacturer's protocol. Briefly, POx (10 mg/mL, 0.5 mL in PBS) was treated with AF647-NHS ester and stirred for 2 h at room temperature in the dark. Labeled POx was separated from free dye by gel filtration (First Bio-Rad BioGel P-30 resin in PBS, then Sephadex LH20 in methanol). The calculated labeling degree was about 25% according to the method in protocol. Next PTX (BODIPY FL PTX:PTX = 1:40) and 17-AAG were coloaded into AF647 labeled POx micelles (no dilution with unlabeled POx) according to the method of section 2.2.1. CLSM was carried out using LSM710 (Carl Zeiss MicroImaging GmbH, Germany). MCF-7 cells were seeded into 4-well plates (Lab-TekII chambered #1.5 German coverglass system) at a density of 40,000 cells per well for 24 h, and then incubated with fluorescently labeled free PTX, polymer alone or POx micelles coloaded with PTX and 17-AAG for 1 and 4 h. Cell nuclei were stained with Hoechst 33342 before CLSM.

### 2.2.8. Cytotoxicity Assay.

MTT (3-[4,5-dimethylthiazol-2-yl]-2,5-diphenyltetrazolium bromide) assay was conducted to evaluate *in vitro* cytotoxicity of drug loaded POx micelles. Briefly, cells were seeded in 96-well plates at a density of 4000 cells/well 24 h prior to drug treatment. Subsequently, cells were treated with micelle-formulated drugs at series of dilutions in full medium. Following 24 h treatment the incubation medium was removed and cells were incubated with fresh medium for another 72 h. The medium was removed and 100 $\mu$L of fresh medium with MTT (100 $\mu$g/well) reagent was added for an additional 3 h incubation at 37 °C. The medium was discarded, the formed formazan salt was dissolved in 100 $\mu$L of DMSO and absorbance was read at 562 nm using a plate reader (SpectraMax M5, Molecular Devices). Cell survival rates were calculated as normalized to control untreated wells. Each concentration was tested in six wells and data presented in means ± standard error means (SEM). The mean drug concentration required for 50% growth inhibition (IC$_{50}$) was determined using CompuSyn software (Version 1.0, Combo-Syn Inc., U.S.) using the median effect equation: $F_a = [1 + (IC_{50}/D)^m]^{-1}$, where $F_a$ is the fraction of affected cells, $D$ is drug concentration and $m$ is the Hill slope.

**Table 1. Solution Concentration, LE and LC of Drugs in POx Aqueous Dispersions ($n = 3 \pm$ SD)[a]**

| drug | soln drug concn (g/L) | LE (%) | LC (%) | total LC (%) | total DL (%) |
|---|---|---|---|---|---|
| PTX | 3.88 ± 0.20 | 97.0 ± 5.1 | 27.9 ± 1.0 | 27.9 ± 1.0 | 38.8 ± 2.0 |
| DTX | 3.87 ± 0.14 | 96.8 ± 3.5 | 27.9 ± 0.7 | 27.9 ± 0.7 | 38.7 ± 1.4 |
| 17-AAG | 3.45 ± 0.21 | 86.2 ± 5.3 | 25.6 ± 1.2 | 25.6 ± 1.2 | 34.5 ± 2.1 |
| ETO | 3.62 ± 0.18 | 90.6 ± 4.6 | 26.6 ± 1.0 | 26.6 ± 1.0 | 36.4 ± 1.9 |
| BTZ | 3.12 ± 0.12 | 77.9 ± 3.1 | 23.8 ± 0.7 | 23.8 ± 0.7 | 31.2 ± 1.2 |
| | | | | | |
| PTX | 3.66 ± 0.15 | 91.6 ± 3.7 | 20.8 ± 0.5 | 43.1 ± 1.2 | 75.9 ± 3.6 |
| 17-AAG | 3.93 ± 0.23 | 98.2 ± 5.6 | 22.3 ± 0.9 | | |
| | | | | | |
| DTX | 3.92 ± 0.10 | 98.1 ± 2.6 | 22.3 ± 0.4 | 43.3 ± 0.6 | 76.3 ± 1.9 |
| 17-AAG | 3.70 ± 0.10 | 92.6 ± 2.5 | 21.0 ± 0.4 | | |
| | | | | | |
| PTX | 3.59 ± 0.33 | 89.8 ± 8.3 | 21.0 ± 1.6 | 41.6 ± 1.6 | 71.4 ± 4.8 |
| ETO | 3.54 ± 0.36 | 88.6 ± 9.0 | 20.7 ± 1.7 | | |
| | | | | | |
| ETO | 3.69 ± 0.17 | 92.2 ± 4.2 | 21.6 ± 0.7 | 41.1 ± 0.9 | 70.7 ± 2.6 |
| 17-AAG | 3.38 ± 0.09 | 84.4 ± 2.2 | 19.8 ± 0.2 | | |
| | | | | | |
| PTX | 3.27 ± 0.33 | 81.6 ± 8.3 | 19.4 ± 1.2 | 40.3 ± 2.4 | 67.8 ± 7.0 |
| BTZ | 3.52 ± 0.38 | 87.9 ± 9.5 | 20.9 ± 1.4 | | |
| | | | | | |
| BTZ | 3.27 ± 0.13 | 81.8 ± 3.2 | 19.8 ± 0.7 | 39.5 ± 0.7 | 65.2 ± 2.1 |
| 17-AAG | 3.25 ± 0.17 | 81.3 ± 4.3 | 19.7 ± 0.9 | | |
| | | | | | |
| PTX | 3.01 ± 0.12 | 75.4 ± 3.0 | 15.5 ± 0.3 | 48.7 ± 1.1 | 94.8 ± 4.0 |
| 17-AAG | 3.19 ± 0.16 | 79.9 ± 4.1 | 16.4 ± 0.6 | | |
| ETO | 3.27 ± 0.16 | 81.8 ± 3.9 | 16.8 ± 0.6 | | |
| | | | | | |
| PTX | 3.18 ± 0.14 | 79.5 ± 3.5 | 16.4 ± 0.5 | 48.4 ± 0.7 | 93.8 ± 2.7 |
| 17-AAG | 3.03 ± 0.11 | 75.7 ± 2.7 | 15.6 ± 0.3 | | |
| BTZ | 3.17 ± 0.03 | 79.4 ± 0.7 | 16.4 ± 0.2 | | |
| | | | | | |
| DTX | 40.60 ± 3.61 | 81.2 ± 7.2 | 44.8 ± 2.2 | 44.8 ± 2.2 | 81.2 ± 7.2[b] |
| PTX | 38.71 ± 2.62 | 77.4 ± 5.2 | 43.6 ± 1.6 | 43.6 ± 1.6 | 77.4 ± 5.3[c] |

[a]Unless stated otherwise, the POx copolymer [P(MeOx$_{40}$-$b$-BuOx$_{21}$-$b$-MeOx$_{34}$)] was used and its concentration in the dispersion was 10 g/L. [b]50 g/L POx and DTX was used in this experiment. [c]50 g/L POx and PTX was used along with a different batch of POx copolymer [P(MeOx$_{33}$-$b$-BuOx$_{26}$-$b$-MeOx$_{45}$)].

### 2.2.9. Combination Index (CI) Analysis.

CI analysis based on the Chou and Talalay method was performed using CompuSyn software.[31] Briefly, for each level of $F_a$ the CI values for binary drug combinations were calculated according to the following equation: CI $= (D)_1/(D_x)_1 + (D)_2/(D_x)_2$, where $(D)_1$ and $(D)_2$ are the concentrations of each drug in the combination resulting in $F_a \times 100\%$ growth inhibition, and $(D_x)_1$ and $(D_x)_2$ are the concentrations of the drugs alone resulting in $F_a \times 100\%$ growth inhibition.[31,32] CI values for drug combinations were plotted as a function of $F_a$. Generally, the CI values between $F_a = 0.2$ and $F_a = 0.8$ are considered valid. The best-fit CI value at IC$_{50}$ was used to show and compare the synergistic effects of drug combinations with different drug ratios or for different cell lines. CI values less than 1 or more than 1 demonstrate synergism or antagonism of drug combinations, respectively.

## 3. RESULTS

### 3.1. Preparation and Characterization of Drug Loaded POx Micelles.

A film hydration method (from ethanol) was used to prepare drug loaded polymeric micelles of POx triblock copolymers, P(MeOx$_{40}$-$b$-BuOx$_{21}$-$b$-MeOx$_{34}$ (batch 1, $M_n = 9.1$

kg/mol, Đ$_M$ = 1.14) and P(MeOx$_{33}$-$b$-BuOx$_{26}$-$b$-MeOx$_{45}$ (batch 2, $M_n = 10.0$ kg/mol, Đ$_M$ = 1.14). According to this method first the drug(s) were blended with the block copolymer and dried, and then the blend was redispersed in water. The incorporation of drugs in micelle dispersions was validated by attenuated total reflectance Fourier transform infrared (ATR FT-IR) spectroscopy (Figure S2 in the Supporting Information) and quantified by HPLC (Table 1). First, in line with our previous account we were able to dissolve 3.9 g/L of PTX and DTX in 10 g/L copolymer (Table 1). Furthermore, we were able to obtain stable micellar solutions of nearly 40 g/L PTX and DTX in 50 g/L copolymer in both distilled water and PBS, which is approximately 100,000 and 7,000 times more than the solubilities of these drugs alone (0.0005 g/L[33] and 0.0055 g/L[13] for PTX and DTX, respectively) (Table 1). In subsequent experiments comparing different drugs and drug mixtures we kept the POx and drug concentrations constant (10 g/L and 4 g/L, respectively) while preparing the solutions. Under these conditions 3.45 ± 0.21 g/L 17-AAG, 3.62 ± 0.18 g/L ETO and 3.12 ± 0.12 g/L BTZ were solubilized as single drugs (Table 1). These apparent solubility values again greatly exceed the
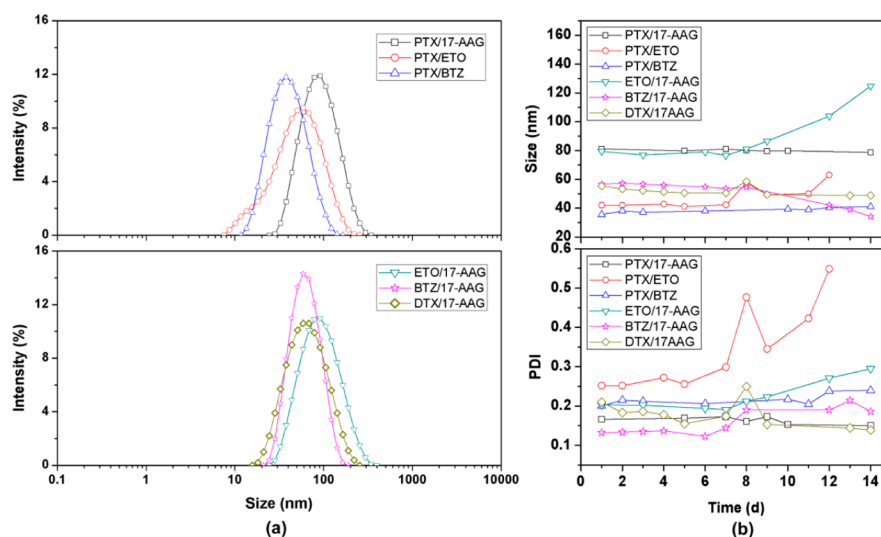
**Figure 2.** (a) Size distribution of POx micelles coloaded with two drugs: PTX/17-AAG (□), PTX/ETO (○), PTX/BTZ (△), ETO/17-AAG (▽), BTZ/17-AAG (☆) and DTX/17-AAG (◇) by DLS. (b) Stability studies of POx micelles coloaded with two drugs as in panel a by plotting average size (nm) and PDI over consecutive time points (days). Lines between data points are for illustration purpose only.

inherent solubility of the drugs alone (0.01 g/L 17-AAG,[34] 0.058 g/L ETO[13] and 0.002−0.004 g/L BTZ[35]).

From the standpoint of the loading efficiency (LE), i.e., the fraction of the drug incorporated into micelles vs total drug added to the system, the PTX and DTX appeared to be favorable having LE values of about 97%. The ETO and 17-AAG displayed LE values of about 91% and 86%, respectively, while BTZ had lower but very good LE of 78%. Another key measure of drug solubilization is the loading capacity (LC), i.e., the fraction by weight of the solubilized drug vs the weight of the entire dispersed phase. In agreement with our previous finding,[14] LC for PTX alone could reach as much as 45%. Moreover, the same high LC value of 45% was achieved for DTX. Thus a very small amount of polymer excipient was needed to solubilize these drugs, which are normally very challenging from the standpoint of formulation. Remarkably, very high LC values were also observed for drug combinations (Table 1). Thus, PTX or DTX in combination with 17-AAG displayed the highest total LC values for binary drug combinations of about 43% (and over 90% LE for each drug). ETO combinations with PTX or 17-AAG also showed over 41% LC and nearly 90% LE. The LC values of the binary combinations comprising BTZ (PTX/BTZ and 17-AAG/BTZ) were slightly lower but still approached 40%. Finally, the ternary drug combinations PTX/17-AAG/ETO and PTX/17-AAG/BTZ displayed very high total LC of about 48 to 49% and LE of ca. 80% for each drug (Table 1). That means that only about 1 g of POx copolymer is needed to solubilize 1 g of such drug mixtures.

The yields of drug-loaded micelles were about 90−99% for single drug, binary or ternary drug combinations as shown in Table S1 in the Supporting Information. The yield of the blank micelles should be 100% since water solubility of the polymers is above 150 g/L and there is no loss of polymer during rehydration of the thin film.

**3.2. Size Distribution and Stability of Drug-Loaded POx Micelles.** The size distribution and dispersion stability of the drug-loaded POx micelles are crucial factors for their successful parenteral application. We measured the particle sizes in the dispersions of the drug loaded micelles using DLS

and examined the size alterations over various periods of time. The micelles loaded with the single drugs, PTX, DTX or 17-AAG, had small hydrodynamic diameters, 36, 18 and 33 nm, and moderate size distributions (PDI), 0.26, 0.30 (bimodal) and 0.18, respectively. The DLS profiles of the micelles loaded with ETO or BTZ were bi- or multimodal with broad size distributions suggesting formation of heterogeneous particle populations (Figure S3a in the Supporting Information). By analyzing these data along with the dispersion stability profiles, we noticed that the larger sizes and broader size distribution patterns of the ETO- and BTZ-loaded micelles were accompanied with their lower stability compared to the micelles loaded with any of the three other drugs. To be more specific, micelles loaded with ETO or BTZ started precipitating after 2 days. In contrast the more uniform and smaller micelles loaded with PTX or 17-AAG remained stable for at least 14 days (Figure S3b in the Supporting Information). This excellent stability combined with relatively small PDI values suggested that the PTX or 17-AAG loaded micelles were thermodynamically stable.

Interestingly, the micelles with binary drug combinations containing either ETO or BTZ coloaded with PTX exhibited more uniform size distribution compared to micelles loaded with ETO or BTZ alone. Their hydrodynamic diameters were 42 and 36 nm and PDI values 0.25 (bimodal) and 0.20, respectively. A similar trend was observed for the micelles containing combinations of either ETO or BTZ with 17-AAG, which also were more homogeneous than the micelles with ETO or BTZ alone. The hydrodynamic diameters of these micelles were 79 and 57 nm and PDI values 0.20 and 0.13, respectively (Figure 2a). Furthermore, micelles with binary drug combinations containing either PTX or 17-AAG exhibited high stability similar to stability of single-drug micelles loaded with PTX or 17-AAG. For example, the ETO/PTX, BTZ/PTX and ETO/17-AAG micelles did not change size for 14 days and BTZ/17-AAG micelles had constant size for 7 days (Figure 2b). Finally, micelles loaded with ternary drug combinations PTX/17-AAG/ETO and PTX/17-AAG/BTZ had hydrodynamic diameters of ca. 53 and 99 nm and relatively small PDI values
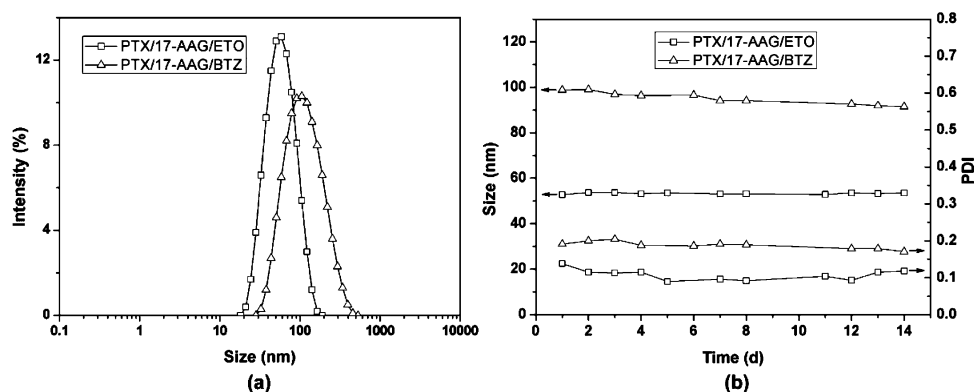
**Figure 3.** (a) Size distribution of POx micelles coloaded with three drugs: PTX/17-AAG/ETO (□) and PTX/17-AAG/BTZ (△). (b) Stability studies of POx micelles coloaded with three drugs as in panel a by plotting average size (nm) and PDI over consecutive time points (days). Lines between data points are for illustration purpose only.
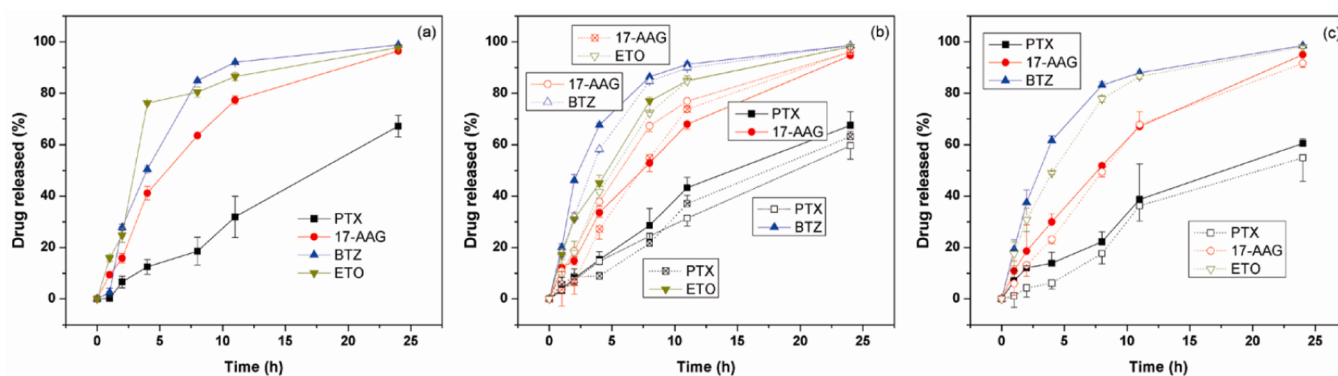


**Figure 4.** *In vitro* drug release from POx micelles for (a) single drug, (b) binary and (c) ternary drug combinations. Drug formulations used in these studies are presented in Table 1 (10 g/L POx).
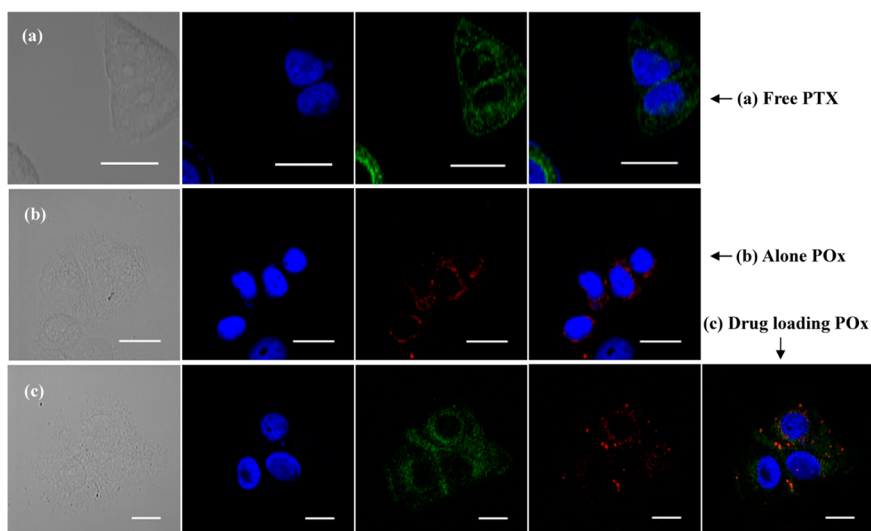


**Figure 5.** CLSM images of MCF-7 cells incubated for 1 h with free (a) PTX, (b) POx copolymer alone and (c) POx micelles coloaded with PTX and 17-AAG. Blue: Cell nuclei staining by Hoechst 33342. Green: BODIPY FL PTX. Red: AF647 labeled POx. Scale bars are 20 $\mu$m.

(0.14 and 0.19, respectively) (Figure 3a). Both dispersions were stable for at least 14 days (Figure 3b).

**3.3. Morphology of Drug-Loaded POx Micelles.** The morphologies of PTX, 17-AAG or PTX/17-AAG loaded micelles were investigated by AFM. In all cases the observed surface-adhered particles were nearly round-shaped (Figure S4 in the Supporting Information). Their average diameters were

28 $\pm$ 14, 20 $\pm$ 12 and 43 $\pm$ 22 nm for PTX-, 17-AAG- and PTX/17-AAG-loaded micelles, respectively. Thus, corroborating the size increase as observed by DLS (Figure 2, Figure S4 in the Supporting Information), AFM reveals larger particles in the PTX/17-AAG formulations as compared to the single drug formulation particles. As commonly observed, the sizes of micellar aggregates determined by AFM were somewhat smaller
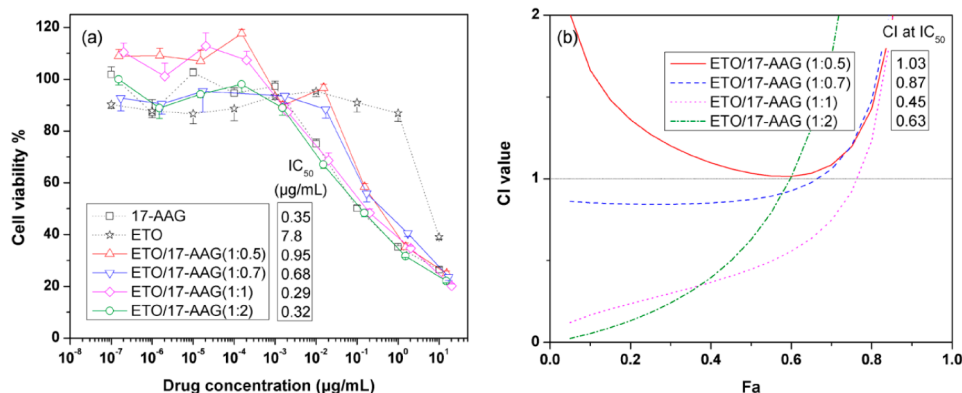
**Figure 6.** (a) Cytotoxicity of single drugs and binary drug combination, ETO/17-AAG solubilized with POx micelles in MCF-7 cells (mean $\pm$ SEM, $n$ = 6) and (b) the corresponding CI vs $F_a$ plot. Please note, the total drug concentration is presented. The $IC_{50}$ values for single micellar ETO and 17-AAG were 7.8 and 0.35 $\mu$g/mL, respectively. At the optimum ratio 1:1 the ETO/17-AAG combination displays $IC_{50}$ = 0.29 $\mu$g/mL (total drug, 0.143 $\mu$g/mL ETO and 0.147 $\mu$g/mL 17-AAG) and CI = 0.45. Dilutions were prepared from stock solutions containing 10 g/L POx, respective drug concentrations were: 3.50 (ETO) and 1.87 (17-AAG) g/L (1:0.5); 3.83 (ETO) and 2.75 (17-AAG) g/L (1:0.7); 3.72 (ETO) and 3.82 (1-AAG) g/L (1:1); 1.85 (ETO) and 3.66 (17-AAG) g/L (1:2).
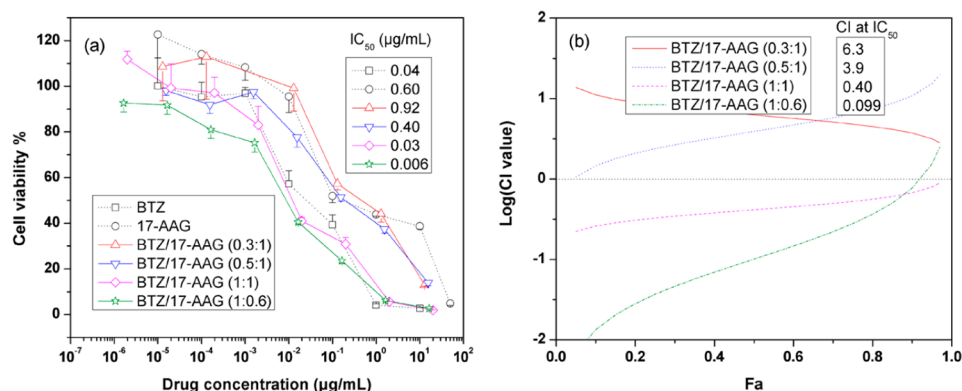


**Figure 7.** (a) Cytotoxicity of single drugs and binary drug combinations, BTZ/17-AAG solubilized in POx micelles in MCF-7 cells (mean $\pm$ SEM, $n$ = 6), and (b) the corresponding log CI vs $F_a$ plot. Note that the total drug concentrations are presented. The $IC_{50}$ values for single micellar BTZ and 17-AAG were 0.04 and 0.6 $\mu$g/mL, respectively. At the optimum ratio (1:0.6) the BTZ/17-AAG combination displays $IC_{50}$ = 0.006 $\mu$g/mL (total drug, 0.00365 $\mu$g/mL BTZ and 0.00235 $\mu$g/mL 17-AAG) and CI = 0.099. Dilutions were prepared from stock solutions containing 10 g/L POx, respective drug concentrations were: 1.040 (BTZ) and 3.58 (17-AAG) g/L (0.3:1); 1.80 (BTZ) and 3.27 (17-AAG) g/L (0.5:1); 3.27 (BTZ) and 3.25 (1-AAG) g/L (1:1); 3.02 (BTZ) and 1.95 (17-AAG) g/L (1:0.6).

compared to DLS results, which can be attributed to the fact that AFM analysis is performed under ambient (dry) conditions while DLS determines the hydrodynamic diameter ("equivalent sphere diameter"), i.e., the size of swollen and hydrated particle in an aqueous phase.[36]

**3.4. In Vitro Drug Release.** The drug release profiles for single, double and triple drug-loaded POx micelle formulations are presented in Figure 4, and the release characteristics corresponding to these profiles are quantified in Table S2 in the Supporting Information. As seen from these data, there was no clear correlation between the drug release rates and drug solubility. Although the least soluble drug, PTX, was also the slowest drug released, another quite poorly soluble drug, BTZ, was released nearly as fast or even faster than the more soluble 17-AAG or ETO. For single drug-loaded formulations about 67% of PTX, 96% of 17-AAG, 99% of BTZ and 98% of ETO were released during the first 24 h (Table S2 in the Supporting Information). Notably there was no burst release observed with any of the single or multiple drug loaded POx micelles. It is also interesting that with few if any exceptions the individual drug release rates practically did not change for double or ternary drug formulations compared to the single drug-loaded POx

micelles. One exception was BTZ that was released twice faster ($t_{1/2}$ = 2 h) from POx micelles containing two drugs, PTX/BTZ compared to the single drug containing micelles ($t_{1/2}$ = 4 h).

**3.5. Internalization of Drug-Loaded in POx Micelles.** The BODIPY FL PTX and AF647-labeled POx block copolymer were used to examine drug and block copolymer internalization and colocalization in MCF-7 cells by CSLM. As shown in Figure 5a, after 1 h incubation the free PTX was distributed in cytoplasm. In contrast the labeled copolymer appeared to be primarily localized in the perinuclear region and mainly, but not exclusively, localized in vesicular bodies (Figure 5b). This distribution pattern did not change significantly for the drug-loaded micelles (Figure 5c). There was little colocalization of drug and polymer albeit the drug appeared to be concentrated around the vesicles and/or some other subcellular compartments, in which the polymer was also present. This may indicate that the drug-loaded micelles serve as intracellular drug depots, from which the drugs are released over time. However, the rate of the release is probably faster than the observation time since the overall distribution pattern did not change significantly after 4 h exposure of the same
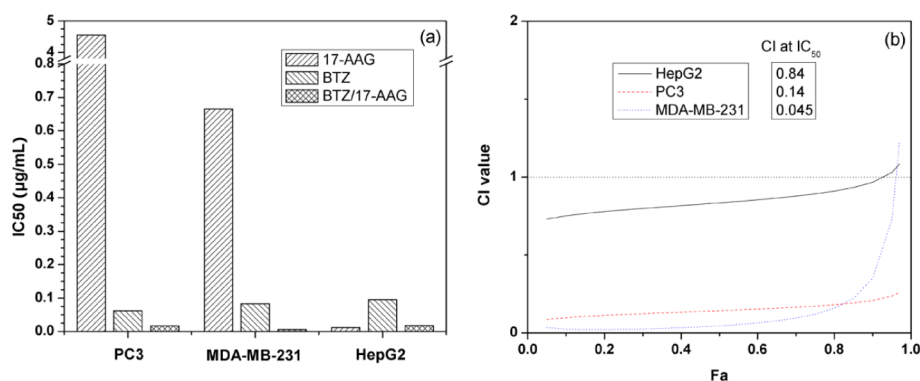
**Figure 8.** (a) IC$_{50}$ values of micellar 17-AAG, BTZ and BTZ/17-AAG combination in PC3, MDA-MB-231, and HepG2 cancer cells and (b) the CI vs $F_a$ plot. The micellar BTZ/17-AAG combination was examined at a 1:1.05 ratio (POx, 10 g/L; BTZ, 4.13 g/L; 17-AAG, 3.78 g/L).

formulation to the cells (Figure S5 in the Supporting Information). Comparing the time scale of this experiment with the time scales observed in the release studies one may conclude that the intracellular release of the drug is faster than its release in the surrounding solution.

**3.6. In Vitro Cytotoxicity and Analysis of Synergistic Effects of Drug Combinations.** The toxicity of POx block copolymer alone was determined in MCF-7, PC-3, HepG2 and MDA-MB-231 cells using MTT assay. In all cell lines, the copolymer displayed little if any toxicity up to the concentration of 200 $\mu$g/mL (Figure S6 in the Supporting Information). To exclude any cytotoxic action of the copolymer on cells, the POx concentration used in subsequent experiments did not exceed 40 $\mu$g/mL. The cytotoxicity of drug combinations solubilized in POx micelles was determined using MCF-7 breast adenocarcinoma cells. Previous reports have demonstrated synergistic cytotoxicity of PTX and 17-AAG in this as well as several other cancer models.[37] Therefore, we analyzed the effects of the other binary drug combinations ETO/17-AAG and BTZ/17-AAG at different drug weight ratios. The first combination, ETO/17-AAG, showed clear synergy at a 1:1 ratio, limited synergy (up to $F_a = 0.6$) at a 1:2 ratio, but little synergy or antagonism at 1:0.5 and 1:0.7 ratios (Figure 6). The second combination, BTZ/17-AAG, displayed strong synergy at 1:0.6 and 1:1 ratios and antagonism at 0.5:1 and 0.3:1 ratios (Figure 7).

Since the BTZ/17-AAG combination displayed very pronounced synergistic cytotoxicity in the MCF-7 cancer cell line, we further evaluated this combination in the human prostate cancer, PC3, triple negative human breast carcinoma, MDA-MB-231, and human hepatocellular carcinoma, HepG2 (Figure S7 in the Supporting Information). While this combination (at a 1.1:1 ratio) displayed little synergy in HepG2 cells, in both PC3 and MDA-MB-231 cells the synergy was very pronounced (Figure 8). Specifically, the IC$_{50}$ values of micellar BTZ, 17-AAG and BTZ/17-AAG formulations were 0.062, 4.6 and 0.017 $\mu$g/mL for PC3 cells, 0.083, 0.67 and 0.006 $\mu$g/mL for MDA-MB-231 cells, and 0.095, 0.012 and 0.018 $\mu$g/mL for HepG2 cells. The corresponding CI values of micellar BTZ/17-AAG combination at IC$_{50}$ were 0.14, 0.045 and 0.84 for PC3, MDA-MB-231 and HepG2 cells, respectively. Unexpectedly, in the multidrug resistant (MDR) human breast adenocarcinoma, MCF-7/ADR, the micellar BTZ/17-AAG combination (0.9:1) displayed an antagonistic effect with a CI value at IC$_{50}$ of 2.1 (Figure S8 in the Supporting Information). In this case the IC$_{50}$ values of micellar 17-AAG, BTZ and BTZ/17-AAG combination were 26, 0.2 and 0.5 $\mu$g/mL, respectively.

## 4. DISCUSSION

Early publications using polymeric micelles with noncovalently incorporated ("solubilized") drugs go back more than two decades,[38] and this technology has undergone clinical evaluation.[39] Separately, combinations of different anticancer drugs in one polymeric vehicle, such as liposomes, nanoparticles or polymer conjugates, have been explored for some time.[11,12,40] However, multiple drug combinations cosolubilized in polymeric micelles were reported relatively recently by the group of Kwon.[13,37] Although polymeric micelles are extremely attractive vehicles due to simplicity of preparation and no need of chemical modification of the drug molecules, achieving high loading capacities has been challenging especially for very poorly soluble drugs. This also was a serious obstacle for developing multidrug combinations in single polymeric micelles. Therefore, recent discovery of high capacity POx micelles that can solubilize such poorly soluble drugs as PTX using nearly 100 times less excipient than the commercial Taxol and 10 times less than Abraxane is a major breakthrough.[14] For comparison, using PEG-*b*-PLA micelles Kwon et al.[13] reported PTX solubility of 3.54 g/L with LC of ca. 9.3% (note that these authors present data for *DL*, which are recalculated in LC in Table S3 in the Supporting Information). In contrast, using POx micelles we report therein PTX solubility of 38.7 g/L with LC of 43.6%. Thus, over ten times more drug was solubilized with only 50 g/L POx block copolymer compared to 30 g/L PEG-*b*-PLA. Furthermore, in the present study extending our previous results POx micelles were shown to have excellent capacity for solubilization of several other poorly soluble drugs, such as DTX, 17-AAG, ETO and BTZ, and their combinations.

The advantages of the POx micelles compared to other polymeric micelle drug delivery systems are clearly seen with several single drugs reported here for the first time. Thus, 10 g/L POx block copolymer was sufficient to solubilize 3.45 g/L 17-AAG with LC of 25.6%. Nearly the same amount of this drug (3.9 g/L) was solubilized with as much as 30 g/L PEG-*b*-PLA (LC 10.2%).[13] For ETO these values were 3.62 g/L ETO in 10 g/L POx (LC 26.6%) vs 3.31 g/L ETO in 30 g/L PEG-*b*-PLA (LC 8.7%).[13] For DTX: 3.87 g/L DTX in 10 g/L POx (LC 27.9%) or 40.6 g/L DTX in 50 g/L POx (LC 44.8%) vs 3.31 g/L DTX in 30 g/L PEG-*b*-PLA (LC 10.3%).[13]

Furthermore, the efficacies of solubilization of the drug blends in POx micelles were similar to or better than those

observed for single drugs. For example, as the initial drug feed increased from 4 g/L (single drug) to 8 g/L (binary drug combinations), and then to 12 g/L (ternary drug combinations), the total LC was also increased from 23.8−27.9% to 39.5−43.3% and up to 48.4−48.7% (POx concentration 10 g/L). This compares favorably to other micellar or liposomal multidrug formulations described in the literature. For example, Kwon et al. used 30 g/L PEG-*b*-PLA copolymer to solubilize a two-drug mixture of 3.9 g/L PTX and 3.9 g/L 17-AAG at total LC of 20.6%.[13] Again, essentially the same concentrations of these drugs were dissolved with 3 times less (10 g/L) POx block copolymer (total LC 43.1%). The same amount of this block copolymer solubilized 3.7 g/L ETO and 3.4 g/L 17-AAG (total LC 41.1%) vs 3.5 g/L ETO and 4.2 g/L 17-AAG solubilized in 30 g/L PEG-*b*-PLA copolymer (total LC 20%).[13] Another direct comparison is a ternary drug combination of 3.5 g/L PTX, 3.6 g/L 17-AAG and 3.2 g/L ETO solubilized using 30 g/L PEG-*b*-PLA block copolymer at total LC of 26.2%.[13] Nearly the same concentrations of these drugs are solubilized with only 10 g/L POx block copolymer (total LC of 48.7%).

Needless to say the drug solubilization capacities of POx micelles are superior not only to PEG-*b*-PLA micelles but also to other multidrug-loaded delivery systems. For example, CSO-SA micelles incorporated PTX and DOX with LC of only about 5.72 wt % (PTX, 4.20%; DOX, 1.52%).[10] Hou et al.[11] prepared VCR and VRP coloaded in PLGA nanoparticles at a total LC of 7.9%. Chiu et al.[12] developed an original multidrug liposomal formulation comprising egg sphingomyelin/cholesterol/PEG2000 ceramide/quercetin coencapsulating quercetin in lipid bilayer and vincristine in aqueous core. The optimal formulation contained about 5 mol % quercetin, and the molar ratio of vincristine to quercetin was 2:1, suggesting that total LC was about 13−14%.

In addition to the high loading capacity the POx micelle formulations displayed high stability.[13] In many cases reported herein, no drug precipitation or changes in the particles sizes for as long as two weeks were observed. For comparison, PTX solubilized in PEG-*b*-PLA block copolymer micelles under similar conditions precipitated in only 24 h.[13] The single drug POx micelle formulations containing ETO or BTZ were more disperse and least stable compared to other drug formulations as they exhibited particle size increase and aggregation started after two to four days. However, when these drugs were blended in binary or ternary drug combinations in POx micelles, the stability of the formulations was markedly improved and they displayed more uniform particle sizes compared to single drug formulations. Noteworthy, Kwon et al. also demonstrated a similar synergistic improvement in stabilities of multidrug loaded PEG-*b*-PLA micelles.[13,37] These authors speculated that such increased stability is due to favorable drug−drug molecular interactions in the multiple drug-loaded micelles. Albeit hypothetical, such an assumption also seems to be the most reasonable explanation for the observed phenomena in our case. On the other hand, in such a case, one might expect a significant effect of drug release upon cosolubilization, which we did not observe. We also hypothesize that high capacity and stability of the drug-loaded POx micelles can be attributed in part to H-bonding between amide bonds of the BuOx block and the H-bond donors in the drug molecules incorporated in the micelle cores. However, using the described experimental setup, no conclusive evidence was obtained at this time by ATR-IR.

Altogether, POx micelles exhibited greater capacity for drug loading and stability compared to the existing micellar system for every drug studied. A marked increase in the drug loading and decrease in the amount of polymeric excipient needed to solubilize chemotherapeutic drugs in POx micelles is likely to translate to lower excipient-related side effects.[14] In this account POx micelles appear to be an extremely attractive drug delivery system and may have great advantage over current methods potentially increasing the safety of clinical interventions. For instance, the current clinical formulation of PTX, Taxol, contains only 1 wt % of active drug, the remainder of the formulation being Cremophor EL and ethanol, which is known to induce hypersentitive reactions as well as neuro- and nephrotoxicities during iv infusions unless countermeasures are taken.[15−17] In a more current PTX formulation, Abraxane, the drug loading was increased to about 10 wt %, but this technique appears to be challenging from a technological point of view for solubilization of multiple drugs.[41] Dimethyl sulfoxide/lipid or Cremophor EL was employed to solubilize 17-AAG, and PEG-sorbitan monooleate (Tween 80) was used in ETO formulations, which resulted in many incidents in clinical trials such as patients' incompliance (early withdrawal) and serious side effects.[42−45] As a consequence, combination therapy involving such hydrophobic drugs has been restricted so far due to the lack of a versatile and nontoxic delivery system for combined delivery of hydrophobic drugs. In this regard low toxicity of POx may be an additional advantage. Early studies on the toxicity of PEtOx reported a very high acute oral $LD_{50}$ of >4 g/kg (rats) and acute percutaneous absorption $LD_{50}$ of >4 g/kg (rabbit).[46] Viegas et al.[21] recently showed that PEtOx is essentially nontoxic when administered iv into rats at amounts of 2 g/kg. Also, repeated administration of 50 mg/kg did not reveal any adverse effects. Our own studies on the biodistribution and excretion using radiolabled PMeOx and PEtOx homopolymers showed a fast distribution of the hydrophilic homopolymers throughout the entire organism (mice) as well as a very rapid renal excretion.[27] Taking together the safety, biodistribution and excretion data for POx polymers, one might hope that they can be advanced to the pharmaceutical sector to develop a versatile drug delivery platform.

To further support our rationale for development of multidrug loaded POx micelles, we studied the tumor cell growth inhibition using selected drug combination and various drug ratios. The studies revealed that synergistic effects can indeed be achieved using ETO/17-AAG and BTZ/17-AAG binary drug formulations and that this effect is strongly influenced by the drug ratio and cell lines used. As discussed previously,[7,47] any synergistic effect greatly depends on drug dosages, combination ratios, cell lines and intervention schedules. For example, 17-AAG is effective in treating solid malignancies and leukemia through inhibiting heat shock protein 90 (HSP90), a chaperone, which interferes with misfolding of various oncogenic proteins.[48] Using a H358 human non-small-cell lung cancer xenograft model, Nguyen et al.[49] found that 17-AAG conferred 5- to 22-fold increase in antitumor efficacy when combined with PTX, a drug that inhibits tumor cell division by stabilizing microtubuli. 17-AAG was also able to suppress FMS-like tyrosine kinase 3 (FLT3), a client of HSP90 whose mutations as internal tandem duplications (ITD) often correlate with poor prognosis.[50] In IDT mutated-FLT3 leukemia cells, DNA-repairing related proteins such as Rad51 and checkpoint kinase 1 (Chk1) were

underexpressed, making them sensitive to ETO, a topoisomerase II antagonist. Therefore, coadministration of 17-AAG and ETO can be synergistic for suppressing leukemia cells specifically with ITD mutated-FLT3. Indeed, we observed a strong synergy of the binary drug combination ETO/17-AAG for selected drug ratios.

Another synergistic binary combination reported in our study is BTZ/17-AAG. BTZ has been approved to treat multiple myeloma. It inhibits the proteasome machinery undermining the cancer cell ability to eliminate aberrant proteins and thus evade apoptotic checkpoints.[51] Combination of BTZ with PTX delayed the tumor growth and achieved high tumor-inhibitory effects on Lewis lung carcinoma.[52] Mimnaugh et al.[53] combined 17-AAG with BTZ and found significant inhibition of breast cancer cell proliferation that was superior to either drug used alone. Apart from the mechanism basis, such synergistic effects depend strongly on optimized ratios of combined drugs, so that synergism may be observed at molar drug ratios that differ significantly from unity.[7,47] For example, codelivery of camptothecin and doxorubicin to glioma cells at a molar ratio of 1.5:1 resulted in synergistic activity, whereas strong antagonism was observed at a ratio of 5:1.[47] Similarly, in our study both binary drug combinations ETO/17-AAG and BTZ/17-AAG were synergistic at some drug ratios but were additive or antagonistic at the other ratios. Therefore, optimization of the drug dosages and ratios in POx micelles will be further considered for combination therapy studies in appropriate disease models using the presented POx codelivery platform. It is worth pointing out that in view of considerable differences between the cell culture and animal model experiments the optimization of the drug ratios may not be a trivial task and would require understanding of the pharmacokinetics and pharmacodynamics of each individual drug in the multidrug composition. Furthermore, translating the results of such laboratory studies to the clinical treatment regimens is always challenging and will be greatly helped by thorough understanding of the absorption, distribution, metabolism, and excretion (ADME) of the multidrug containing polymeric micelles.

Finally, the chemical versatility[18,54] of POx block copolymers can be exploited for the preparation of targeted micelles in the future, potentially increasing the therapeutic opportunities with this high-capacity micelle multidrug delivery platform. The fine-tuning of the amphiphilic contrast of POx monomer units, blocks and the entire polymer should also have direct implementations in the morphology of the micellar aggregates and allow design of the shape and size of these aggregates to match the specific requirements to accommodate a variety of drugs as well as optimize size dependent pharmacokinetics and biodistribution behavior of the carrier.[55−61]

## 5. CONCLUSIONS

In conclusion, we have shown that POx micelles are able to incorporate large amounts of different hydrophobic anticancer agents. In addition, this carrier system also provides means for the realization of highly stable and well-defined binary and ternary drug formulations with unprecedented high drug loading. Interestingly, binary and ternary drug formulations display improved stability and reduced dispersity compared to the single drug containing micelles. The multidrug loaded micelles can deliver drugs to cancer cells and display synergistic effects against several tumor models. These synergistic effects were dependent on drug ratios, which require further

optimization of the corresponding multidrug formulations. Altogether the multidrug loaded POx micelles represent an attractive platform for further development of combination anticancer therapeutics.

## ■ ASSOCIATED CONTENT

### ⓢ Supporting Information

Chemical structures of anticancer drugs; attenuated total reflectance Fourier transform infrared (ATR FT-IR) spectra of amphiphilic block copolymer alone, and POx block copolymer micelles loaded with PTX, 17-AAG and combination of PTX and 17-AAG; size distribution (DLS) of POx micelles loaded with single drugs (PTX, 17-AAG, DTX, ETO, BTZ) and stability over consecutive time points; AFM topography scans of drug-loaded micelles of POx; CLSM images of MCF-7 cells incubated with free PTX, POx block copolymer alone and POx micelles coloaded with PTX and 17-AAG for 4 h; the viability of the MCF7, MDA-MB-231, HepG2 and PC3 cells after their treatment for 24 h to different concentrations of amphiphilic POx block copolymer; the viability of the HepG2, PC3 and MDA-MB-231 cells after their treatment for 24 h with the micellar BTZ, 17-AAG and BTZ/17-AAG combination; cytotoxicity of single drugs and two-drug combination, BTZ/17-AAG solubilized in POx micelles in MCF7/ADR cells; characteristics of the drug release from POx micelles; comparison of our results with others for drug formulation. This material is available free of charge via the Internet at http://pubs.acs.org.

## ■ AUTHOR INFORMATION

### Corresponding Author

*A.V.K.: Center for Drug Delivery and Nanomedicine and Department of Pharmaceutical Sciences, College of Pharmacy, University of Nebraska Medical Center, Omaha, NE 68198-5830, United States; tel, +1 402 559 9364; fax, +1 402 559 9365; e-mail, skabanov@me.com. R.L.: Professur für Makromolekulare Chemie, Department Chemie, Technische Universität Dresden, Zellescher Weg 19, 01069 Dresden, Germany; tel, +49 351 463 36057; fax, +49 351 463 37122; e-mail, robert.luxenhofer@chemie.tu-dresden.de.

### Author Contributions

§Both authors contributed equally to this work.

### Notes

The authors declare no competing financial interest.

## ■ ACKNOWLEDGMENTS

## ■ REFERENCES

(1) Persidis, A. Cancer multidrug resistance. Nat. Biotechnol. 1999, 17, 94−95.

(2) Clarke, M. F.; Fuller, M. Stem cells and cancer: two faces of Eve. Cell 2006, 124, 1111−1115.

(3) Reya, T.; Morrison, S. J.; Clarke, M. F.; Weissman, I. L. Stem cells, cancer, and cancer stem cells. *Nature* **2001**, *414*, 105−111.

(4) Lapidot, T.; Sirard, C.; Vormoor, J.; Murdoch, B.; Hoang, T.; Caceres-Cortes, J.; Minden, M.; Paterson, B.; Caligiuri, M. A.; Dick, J. E. A cell initiating human acute myeloid leukaemia after transplantation into SCID mice. *Nature* **1994**, *367*, 645−648.

(5) Al-Hajj, M.; Wicha, M. S.; Benito-Hernandez, A.; Morrison, S. J.; Clarke, M. F. Prospective identification of tumorigenic breast cancer cells. *Proc. Natl. Acad. Sci. U.S.A.* **2003**, *100*, 3983−3988.

(6) Ramaswamy, S. Rational design of cancer-drug combinations. *N. Engl. J. Med.* **2007**, *357*, 299−300.

(7) Mayer, L. D.; Janoff, A. S. Optimizing combination chemotherapy by controlling drug ratios. *Mol. Interventions* **2007**, *7*, 216−223.

(8) Reddy, N.; Czuczman, M. S. Enhancing activity and overcoming chemoresistance in hematologic malignancies with bortezomib: preclinical mechanistic studies. *Ann. Oncol.* **2010**, *21*, 1756−1764.

(9) Xiao, L.; Rasouli, P.; Ruden, D. M. Possible effects of early treatments of Hsp90 inhibitors on preventing the evolution of drug resistance to other anti-cancer drugs. *Curr. Med. Chem.* **2007**, *14*, 223−232.

(10) Zhao, M. D.; Hu, F. Q.; Du, Y. Z.; Yuan, H.; Chen, F. Y.; Lou, Y. M.; Yu, H. Y. Coadministration of glycolipid-like micelles loading cytotoxic drug with different action site for efficient cancer chemotherapy. *Nanotechnology* **2009**, *20*, 055102.

(11) Song, X.; Zhao, Y.; Wu, W.; Bi, Y.; Cai, Z.; Chen, Q.; Li, Y.; Hou, S. PLGA nanoparticles simultaneously loaded with vincristine sulfate and verapamil hydrochloride: Systematic study of particle size and drug entrapment efficiency. *Int. J. Pharm.* **2008**, *35*, 320−329.

(12) Wong, M.-Y.; Chiu, G. N. C. Simultaneous liposomal delivery of quercetin and vincristine for enhanced estrogen-receptor-negative breast cancer treatment. *Anti-Cancer Drugs* **2010**, *21*, 401−410.

(13) Shin, H. C.; Alani, A. W. G.; Rao, D. A.; Rockich, N. C.; Kwon, G. S. Multi-drug loaded polymeric micelles for simultaneous delivery of poorly soluble anticancer drugs. *J. Controlled Release* **2009**, *140*, 294−300.

(14) Luxenhofer, R.; Schulz, A.; Roques, C.; Li, S.; Bronich, T. K.; Batrakova, E. V.; Jordan, R.; Kabanov, A. V. Doubly amphiphilic poly(2-oxazoline)s as high-capacity delivery systems for hydrophobic drug. *Biomaterials* **2010**, *31*, 4972−4979.

(15) Gelderblom, H.; Verweij, J.; Nooter, K.; Sparreboom, A. Cremophor EL: The drawbacks and advantages of vehicle selection for drug formulation. *Eur. J. Cancer* **2001**, *37*, 1590−1598.

(16) Hennenfent, K. L.; Govindan, R. Novel formulations of taxanes: a review. Old wine in a new bottle? *Ann. Oncol.* **2006**, *17*, 735−749.

(17) Weiss, R.; Donehower, R.; Wiernik, P.; Ohnuma, T.; Gralla, R.; Trump, D.; Baker, J., Jr.; Van Echo, D.; Von Hoff, D.; Leyland-Jones, B. Hypersensitivity reactions from taxol. *J. Clin. Oncol.* **1990**, *8*, 1263−1268.

(18) Barz, M.; Luxenhofer, R.; Zentel, R.; Vicent, M. J. Overcoming the PEG Addiction: well-defined alternatives to PEG, from structure-property relationships to better defined therapeutics. *Polym. Chem.* **2011**, *2*, 1900−1918.

(19) Luxenhofer, R.; Han, Y.; Schulz, A.; Tong, J.; He, Z.; Kabanov, A. V. Poly(2-oxazoline)s as polymer therapeutics. *Macromol. Rapid Commun.* **2012**, DOI: 10.1002/marc.201200354.

(20) Rehfeldt, F.; Tanaka, M.; Pagnoni, L.; Jordan, R. Static and dynamic swelling of grafted poly(2-alkyl-2-oxazoline)s. *Langmuir* **2002**, *18*, 4908−4914.

(21) Viegas, T. X.; Bentley, M. D.; Harris, J. M.; Fang, Z.; Yoon, K.; Dizman, B.; Weimer, R.; Mero, A.; Pasut, G.; Veronese, F. M. Polyoxazoline: Chemistry, properties, and applications in drug delivery. *Bioconjugate Chem.* **2011**, *22*, 976−986.

(22) Foreman, M. B.; Coffman, J. P.; Murcia, M. J.; Cesana, S.; Jordan, R.; Smith, G. S.; Naumann, C. A. Gelation of amphiphilic lipopolymers at the air-water interface: 2D analogue to 3D gelation of colloidal systems with grafted polymer chains? *Langmuir* **2003**, *19*, 326−332.

(23) Lin, P.; Clash, C.; Pearce, E. M.; Kwei, T. K.; Aponte, M. A. Solubility and miscibility of poly(ethyl oxazoline). *J. Polym. Sci., Part B: Polym. Phys.* **1988**, *26*, 603−619.

(24) Chen, F. P.; Ames, A. E.; Taylor, L. D. Aqueous solutions of poly(ethyloxazoline) and its lower consolute phase transition. *Macromolecules* **1990**, *23*, 4688−4695.

(25) Zalipsky, S.; Hansen, C. B.; Oaks, J. M.; Allen, T. M. Evaluation of blood clearance rates and biodistribution of poly (2-oxazoline)-grafted liposomes. *J. Pharm. Sci.* **1996**, *85*, 133−137.

(26) Woodle, M. C.; Engbers, C. M.; Zalipsky, S. New amphipatic polymerelipid conjugates forming long-circulating reticuloendothelial system-evading liposomes. *Bioconjugate Chem.* **1994**, *5*, 493−496.

(27) Gaertner, F. C.; Luxenhofer, R.; Blechert, B.; Jordan, R.; Essler, M. Synthesis, biodistribution and excretion of radiolabeled poly(2-alkyl-2-oxazoline)s. *J. Controlled Release* **2007**, *119*, 291−300.

(28) Huber, S.; Jordan, R. Modulation of the lower critical solution temperature of 2-alkyl-2-oxazoline copolymers. *Colloid Polym. Sci.* **2008**, *286*, 395−402.

(29) Park, J. S.; Kataoka, K. Comprehensive and accurate control of thermosensitivity of poly (2-alkyl-2-oxazoline)s via well-defined gradient or random copolymerization. *Macromolecules* **2007**, *40*, 3599−3609.

(30) Luxenhofer, R.; Sahay, G.; Schulz, A.; Alakhova, D.; Bronich, T. K.; Jordan, R.; Kabanov, A. V. Structure-property relationship in cytotoxicity and cell uptake of poly(2-oxazoline) amphiphiles. *J. Controlled Release* **2011**, *153*, 73−82.

(31) Chou, T.-C. Theoretical Basis, Experimental Design, and Computerized Simulation of Synergism and Antagonism in Drug Combination Studies. *Pharmacol. Rev.* **2006**, *58*, 621−681.

(32) Sain, N.; Krishnan, B.; Ormerod, M. G.; De Rienzo, A.; Liu, W. M.; Kaye, S. B.; Workman, P.; Jackman, A. L. Potentiation of paclitaxel activity by the HSP90 inhibitor 17-allylamino-17-demethoxygeldanamycin in human ovarian carcinoma cell lines with high levels of activated AKT. *Mol. Cancer Ther.* **2006**, *5*, 1197−1208.

(33) Liggins, R. T.; Hunter, W. L.; Burt, H. M. Solid-state characterization of paclitaxel. *J. Pharm. Sci.* **2000**, *86*, 1458−1463.

(34) Development Therapeutics Program of the National Cancer Institute, Geldanamycin analogs. Bethesda, MD: Development Therapeutics Program of the National Cancer Institute. 2007, http://dtp.nci.nih.gov/timeline/posters/AGG_Geldamycin.pdf.

(35) Material safety data sheet for Bortezomib. Revision date: May 20, 2009. LC laboratories.

(36) Solomatin, S. V.; Bronich, T. K.; Bargar, T. W.; Eisenberg, A.; Kabanov, V. A.; Kabanov, A. V. Environmentally responsive nano-particles from block ionomer complexes: Effects of pH and ionic strength. *Langmuir* **2003**, *19*, 8069−8076.

(37) Shin, H. C.; Alani, A. W. G.; Cho, H.; Bae, Y.; Kolesar, J. M.; Kwon, G. S. A 3-in-1 polymeric micelle nanocontainer for poorly water-soluble drugs. *Mol. Pharmaceutics* **2011**, *8*, 1257−1265.

(38) Kabanov, A. V.; Chekhonin, V. P.; Alakhov, V. Y.; Batrakova, E. V.; Lebedev, A. S.; Melik-Nubarov, N. S.; Arzhakov, S. A.; Levashov, A. V.; Morozov, G. V.; Severin, E. S.; Kabanov, V. A. The neuroleptic activity of haloperidol increases after its solubilization in surfactant micelles. Micelles as microcontainers for drug targeting. *FEBS Lett.* **1989**, *258*, 343−345.

(39) Duncan, R. The dawning era of polymer therapeutics. *Nat. Rev. Drug Discovery* **2011**, *2*, 347−360.

(40) Aryal, S.; Hu, C.-M. J.; Zhang, L. Combinatorial drug conjugation enables nanoparticle dual-drug delivery. *Small* **2010**, *6*, 1442−1448.

(41) ABRAXIS BIOSCIENCE, ABRAXANE® for Injectable Suspension (paclitaxel protein-bound particles for injectable suspension), U.S. Food and Drug Administration, http://www.accessdata.fda.gov/drugsatfda_docs/label/2008/021660s013lbl.pdf.

(42) Solit, D. B.; Ivy, S. P.; Kopil, C.; Sikorski, R.; Morris, M. J.; Slovin, S. F.; Kelly, W. K.; DeLaCruz, A.; Curley, T.; Heller, G.; Larson, S.; Schwartz, L.; Egorin, M. J.; Rosen, N.; Scher, H. I. Phase I trial of 17-Allylamino-17-Demethoxygeldanamycin in patients with advanced cancer. *Clin. Cancer Res.* **2007**, *13*, 1775−1782.

(43) Grem, J. L.; Morrison, G.; Guo, X. D.; Agnew, E.; Takimoto, C. H.; Thomas, R.; Szabo, E.; Grochow, L.; Grollman, F.; Hamilton, J. M.; Neckers, L.; Wilson, R. H. Phase I and pharmacologic study of 17-(allylamino)-17-demethoxygeldanamycin in adult patients with solid tumors. *J. Clin. Oncol.* **2005**, *23*, 1885−1893.

(44) Solit, D. B.; Osman, I.; Polsky, D.; Panageas, K. S.; Daud, A.; Goydos, J. S.; Teitcher, J.; Wolchok, J. D.; Germino, F. J.; Krown, S. E.; Coit, D.; Rosen, N.; Chapman, P. B. Phase II trial of 17-allylamino-17-demethoxy-geldanamycin in patients with metastatic melanoma. *Clin. Cancer Res.* **2008**, *14*, 8302−8307.

(45) Hande, K. R. Etoposide: four decades of development of a topoisomerase II inhibitor. *Eur. J. Cancer* **1998**, *34*, 1514−1521.

(46) Kobayashi, S. Ethylenimine polymers. *Prog. Polym. Sci.* **1990**, *15*, 751−823.

(47) Mayer, L. D.; Harasym, T. O.; Tardi, P. G.; Harasym, N. L.; Shew, C. R.; Johnstone, S. A.; Ramsay, E. C.; Bally, M. B.; Janoff, A. S. Ratiometric dosing of anticancer drug combinations: Controlling drug ratios after systemic administration regulates therapeutic activity in tumor-bearing mice. *Mol. Cancer Ther.* **2006**, *5*, 1854−1863.

(48) Ramanathan, R. K.; Egorin, M. J.; Eiseman, J. L.; Ramalingam, S.; Friedland, D.; Agarwala, S. S.; Ivy, S. P.; Potter, D. M.; Chatta, G.; Zuhowski, E. G.; Stoller, R. G.; Naret, C.; Guo, J.; Belani, C. P. Phase I and pharmacodynamic study of 17-(allylamino)-17-demethoxygeldanamycin in adult patients with refractory advanced cancers. *Clin. Cancer Res.* **2007**, *13*, 1769−1774.

(49) Nguyen, D. M.; Lorang, D.; Chen, G. A.; Stewart, J. H., IV; Tabibi, E.; Schrump, D. S. Enhancement of paclitaxel-mediated cytotoxicity in lung cancer cells by 17-allylamino geldanamycin: In vitro and in vivo analysis. *Ann. Thorac. Surg.* **2001**, *72*, 371−379.

(50) Yao, Q.; Weigel, B.; Kersey, J. Synergism between etoposide and 17-AAG in leukemia cells: critical roles for hsp90, FLT3, topoisomerase II, chk1, and rad51. *Clin. Cancer Res.* **2007**, *13*, 1591−1600.

(51) Adams, J. The proteasome: a suitable antineoplastic target. *Nat. Rev. Cancer* **2004**, *4*, 349−360.

(52) Teicher, B. A.; Ara, G.; Herbst, R.; Palombella, V. J.; Adams, J. The proteasome inhibitor PS-341 in cancer therapy. *Clin. Cancer Res.* **1999**, *5*, 2638−2645.

(53) Mimnaugh, E. G.; Xu, W.; Vos, M.; Yuan, X.; Isaacs, J. S.; Bisht, K. S.; Gius, D.; Neckers, L. Simultaneous inhibition of hsp 90 and the proteasome promotes protein ubiquitination, causes endoplasmic reticulum-derived cytosolic vacuolization, and enhances antitumor activity. *Mol. Cancer Ther.* **2004**, *3*, 551−566.

(54) Luxenhofer, R.; Jordan, R. Click chemistry with poly (2-oxazoline)s. *Macromolecules* **2006**, *39*, 3509−3516.

(55) Baekmark, T. R.; Sprenger, I.; Ruile, M.; Nuyken, O.; Merkel, R. Compression-induced formation of surface micelles in monolayers of a poly(2-oxazoline) diblock copolymer at the air-water interface: A combined film balance and electron microscopy study. *Langmuir* **1998**, *14*, 4222−4226.

(56) Bonne, T. B.; Lüdtke, K.; Jordan, R.; Stepanek, P.; Papadakis, C. M. Aggregation behavior of amphiphilic poly(2-alkyl-2-oxazoline) diblock copolymers in aqueous solution studied by fluorescence correlation spectroscopy. *Colloid Polym. Sci.* **2004**, *282*, 833−843.

(57) Bonne, T. B.; Lüdtke, K.; Jordan, R.; Papadakis, C. M. Effect of polymer architecture of amphiphilic poly(2-oxazoline) copolymers on the aggregation and aggregate structure. *Macromol. Chem. Phys.* **2007**, *201*, 1402−1408.

(58) Papadakis, C. M.; Ivanova, R.; Lüdtke, K.; Mortensen, K.; Pranzas, P. K.; Jordan, R. Micellar structure of amphiphilic poly(2-oxazoline) diblock copolymers. *J. Appl. Crystallogr.* **2007**, *40*, 361−362.

(59) Ivanova, R.; Komenda, T.; Bonne, T. B.; Lüdtke, K.; Mortensen, K.; Pranzas, P. K.; Jordan, R.; Papadakis, C. M. Micellar structures of hydrophilic-lipophilic and hydrophilic-fluorophilic poly(2-oxazoline) diblock copolymers in water. *Macromol. Chem. Phys.* **2008**, *209*, 2248−2258.

(60) Hoogenboom, R.; Wiesbrock, F.; Leenen, M. A. M.; Thijs, H. M. L.; Huang, H. Y.; Fustin, C. A.; Guillet, P.; Gohy, J. F.; Schubert, U. S. Synthesis and aqueous micellization of amphiphilic tetrablock ter- and quarterpoly(2-oxazoline)s. *Macromolecules* **2007**, *40*, 2837−2843.

(61) Fustin, C. A.; Lefevre, V.; Hoogenboom, R.; Schubert, U. S.; Gohy, J. F. Micellization of poly(2-oxazoline)based quasi-diblock copolymers on surfaces. *Macromol. Chem. Phys.* **2007**, *208*, 2026−2031.